Low-coherence ESPI in the investigation of ancient terracotta warriors.

Gerd Gülker, Klaus D. Hinsch, Arne Kraft

Carl von Ossietzky University Oldenburg, Department of Physics, P.O.: 2503
26111 Oldenburg, Germany

ABSTRACT

In order to investigate deterioration processes in the paint layers on the famous 2000-yr-old Chinese Terracotta warriors, a low coherence ESPI system was designed. In this modified set-up a short-coherent superluminescence diode instead of a laser is used. By changing the path length of one of the interfering beams it is possible to select a region limited in depth where deformations are measured even if it is below the surface. Results on an artificial test object and on original terracotta fragments demonstrate the limits and the capabilities of the new method.

Keywords: short coherence interferometry; inspection of works of art; spatial phase shifting; microscopic ESPI; OCT

1. INTRODUCTION

Since several years electronic speckle pattern interferometry (ESPI) has proved to be a powerful tool in the real-time observation of micro deformations. Our group uses this technique for the investigation of deterioration processes in works of art and for the development of procedures for their preservation[1]. The aim of investigations on polychrome fragments of the famous 2000-yr-old Chinese Terracotta Army is to estimate the suitability of several conservation agents and procedures, which are developed to preserve the extremely endangered paint layers. To investigate the individual layers of the multi layered painting separately a modified ESPI system was designed with a low-coherent superluminescent diode (SLD) instead of a laser. By changing the path length of one of the interfering beams it is possible to select a region limited in depth where deformations should be measured even if it is located below the surface. The use of spatial phase shifting in combination with the Fourier transform method allows the separation of the coherent from the incoherent part of the reflected light, which is very helpful for a reliable evaluation of the phase maps. We demonstrate deformation measurements on an artificial test object and on terracotta fragments.

2. LOW-COHERENCE ESPI

In order to separate the light from different depth layers of a scattering volume from unwanted background light, a few methods were proposed in recent years. The basic of all these methods is the measuring of the echo time delay and magnitude of backscattered light. One possibility is to use ultra fast shutters like a Kerr shutter as first shown more than 30 years ago[2]. A second possibility is the use of low-coherence interferometry, sometimes called coherence-gated imaging. Here, interference is observed only if the difference in path lengths between reference and object waves is less than the coherence length of the light used in the experiment. A well-known representative of these techniques is optical coherence tomography (OCT)[3], another one is low-coherence holography[4]. Typically, these methods are used to get cross-sectional tomographic images from the internal microstructure in materials and biological systems. Our aim is not (only) to get absolute topographic information about the internal structure but to measure their deformations.

In Fig. 1, a scheme of the used low-coherence ESPI set-up is shown. The underlying basics of standard ESPI are well-known and comprehensively described in literature, e.g.[5]. In this modified set-up, the laser light source is replaced by a superluminescence diode (SLD). It has an output power of 8 mW, a central wavelength of 840 nm and a line width of 20 nm FWHM. The coherence length is about 34 µm, which means the 1/e-value of the contrast function. The object and the reference waves are coupled into single mode fibers. The angle between illumination and observation direction is as small as possible, so that mainly the out-of-plane component of the deformation vector is registered. The end of the fiber, which guided the illumination beam and the collimating lens are mounted on a long range PZT translation stage. This enables us to control the position of the lens and thus the path length of the object beam. A small object region in depth is thus defined, where the paths lengths of the reference and object beams are matched to within the coherence length of the SLD. As a consequence, only light reflected from this region can interfere with the reference beam on the CCD camera. Only from this area, which further on is called coherence region, deformations can be measured. The light

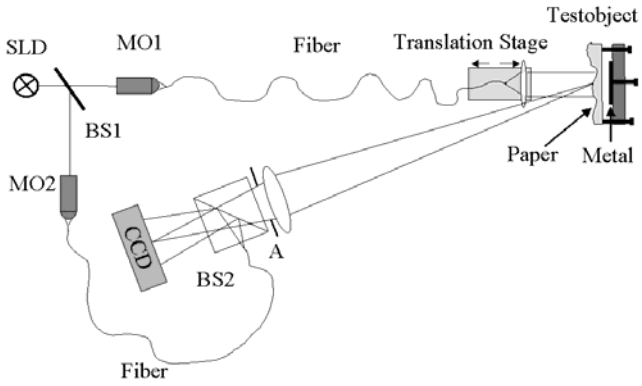

Fig.1. Set-up of low-coherence ESPI (MO: microscope objective; BS: beam splitter; A: aperture)

scattered from all other parts of the object is incoherent with the reference beam and does only contribute to the interference pattern as unwanted background light.

The reference beam is superimposed to the object beam by a beam splitter just in front of the CCD Camera. The virtual source point of the beam is located in the plane of the aperture, but with a well-defined small shift off the center of the aperture. Thus a linear phase shift is generated across the image. If the mean size of the speckles is at least as large as three pixels of the CCD array it is possible to determine three phase shifted values for each individual speckle within the image. Clearly, the continuous phase progression over the CCD sensor leads to an integration over the pixels, so that this procedure represents the integrated bucket method of phase shifting. Instead of extracting the phase from phase-shifted interferograms sequentially recorded in time this so called spatial phase shifting method reveals the phase map of the speckle pattern simultaneously from one single image. During the measuring process phase maps are continuously calculated and subtracted from previous or from the original phase map resulting in mod-2π phase representations of the occurring deformations.

To evaluate the phase maps we use the Fourier transform method. The way to retrieve phase information modulated on a carrier frequency, by means of Fourier Transforms, has been described many years ago[6]. The principles of this method are shown in Fig. 2. In Fig. 2a an initial speckle pattern is shown. Superposition with the laterally shifted reference beam generates carrier fringes within the individual speckles (Fig. 2b). FFT produces the according side lobes (Fig. 2c). In some cases when the intensity of the object light and thus the speckles are very bright as compared with the reference beam the speckle halo in the middle of the Fourier transform will overlap with the side lobes. This can lead to errors in the phase evaluation. To eliminate the speckle halo it is suitable to take a picture of the speckle pattern without the reference beam and subtract this from the interferogram. This leads to a pronounced enhancement in contrast. To evaluate the phase map only a single side lope (circled in Fig. 2d) is selected for the inverse FFT.

The evaluation of the deformations as described by spatial phase shifting and the Fourier Transform method has several advantages. The first one is quite obvious: only coherent light can build up the spatial carrier fringe pattern. By selecting a single side lobe for the inverse FFT we eliminate the unwanted incoherent light, e.g., from the surface of the object. Secondly, if no side lopes appear within the spectrum of the interferogram there is no coherent object light, which can interfere with the reference beam. This means that the object under investigation shows no internal backscattering microstructure within the coherence region. In other words, no light is scattered from the depth selected by the coherence region and, of course, no deformation measurements are possible in this particular object depth. Again, this information can be extracted from a single image without the necessity of scanning the path length of one arm of the interferometer continuously, as for example in standard OCT. Last no least, the Fourier transform method allows not only the calculation of the phase map but also the reconstruction of the intensity of the object light[7], which is reflected within the coherent region. This means that the speckle pattern produced by light scattered within the selected depth region of the object can be calculated as well. This enables us to detect position resolved the magnitude of scattered light from selected object regions, which is identical with a complete two dimensional OCT measurement. The method represents thus intrinsically a 2-D OCT system, too. For deformation measurements the reconstructed speckle

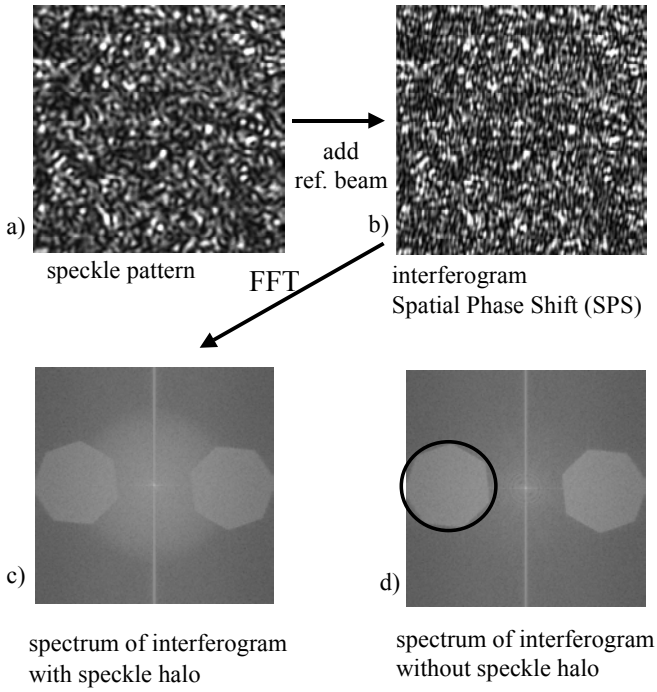

Fig. 2. Principle of the Fourier transform method. To evaluate the phase map and for reconstruction of scattered intensity only the marked circle is used.

pattern is also very important. Parts of the image with pronounced speckle de-correlation or with poor speckle contrast can thus be identified and omitted in the evaluation procedure in order to obtain reliable deformation data.

3. MEASUREMENTS ON ARTIFICIAL TEST OBJECT

To demonstrate the capability of the low-coherent ESPI as compared with the unmodified system measurements were performed on a two-layered artificial test object. This specimen is also schemed in Fig. 1. It consists of two layers, an ordinary piece of paper placed at a variable distance in front of a white painted metal plate. The different layers can be displaced independently: the piece of paper can be tilted and the metal plate can be tilted or dent by a rear screw. Each measurement was carried out with two light sources, the SLD and a long-coherence DBR laser diode. While measuring with the SLD the path lengths are adjusted in such a way that the coherence region firstly is located at the paper surface layer and then at the surface layer of the metal plate. In case of using the laser diode no adjusting of path length is required because the distance between paper and metal plate is much smaller than the coherence length of the laser.

In Fig. 3 some results of this preliminary experiments are shown in a mod-2π phase representation, also called sawtooth images. The size of the investigated area is 4x4 mm^2. On the left side of the figure two images obtained with the long-coherence laser diode are shown, whereas the right side represents two respective results with the SLD. Both upper images of Fig. 3 result from a tilt of the upper paper layer, while the lower images are obtained after denting the lower metal layer. Let us first discuss the upper phase maps. The contrast of the fringes obtained with the SLD is only slightly better than the fringe system obtained with a laser diode. Both fringe systems are degraded possibly due to multiple scattering and due to humidity fluctuations. The fringes obtained with the laser diode suffer in addition from the coherent light scattered by the metal plate, which is incoherent in the low-coherence case and thus less annoying.

More impressive are the effects if the second layer is observed (lower images in Fig. 4). With the laser diode the fringe pattern resulting from the dent are hardly visible (lower left) while the phase map from the SLD experiment shows up with a good contrast (lower right). In this case the scattered incoherent light from the paper does not degrade the fringe contrast. So, the deformation pattern can easily be evaluated.

During our measurements we saw that the degradation of the phase maps of the lower layer depends not only on the amount of reflected light, but also strongly on the amount of deformation of both the layers in respect to each other and

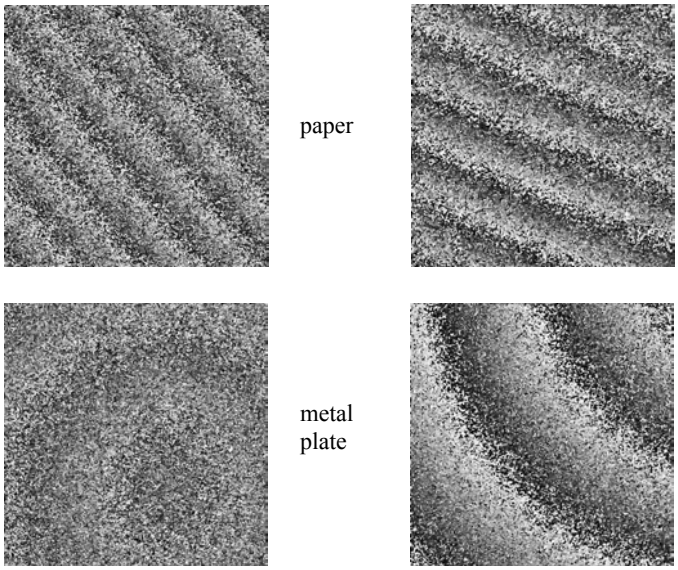

Fig. 3**.** Mod-2π phase maps representing deformation of test object due to tilting the paper (upper) and denting the metal plate (lower). Left: results with laser diode. Right: results with low-coherence SLD.

on the distance between the layers. In order to estimate the limits of the LCSI, measurements were performed on the artificial layered object with different tilts of the two layers and at several distances. For a quantitative comparison of the resulting mod-2π phase maps, a synthetic, noise-free sawtooth image is fitted to the completely unprocessed original ones[8]. The rms deviation $\sigma_{\Delta\varphi}$ is taken as a measure for the degradation. Note that the largest detectable $\sigma_{\Delta\varphi}$ amounts to $\pi/\sqrt{3}$, which is the rms of a uniform distribution within the range [-π,+π]. In this case, the speckle patterns, which are taken before and after loading the object and used to calculate the phase map, are totally de-correlated. In Fig. 4 some results of this measurements are shown. In Fig. 4 left, $\sigma_{\Delta\varphi}$ is shown as a function of the tilt angle of the upper layer for three different distances between both layers. In this case the lower layer remains undeformed. It can be seen, that $\sigma_{\Delta\varphi}$ generally increases with growing tilt angle until its maximum value of about 1,8. In addition, the degradation of the fringe patterns depends on the layer distances: the higher the distance the slower the increase of $\sigma_{\Delta\varphi}$ with respect to the tilt angle.

In Fig. 4 right, the same is shown for the situation, where the lower layer is tilted and the upper one remains untilted. Again, $\sigma_{\Delta\varphi}$ increases with growing tilt angle. But in this case, a higher distance leads to a faster degradation with respect to the tilt angle. A first simple theoretical approach, which only considers path length changes of interfering light rays geometrically due to tilt of the two layers, shows the same principal dependence between $\sigma_{\Delta\varphi}$, tilt angle, and distance of the layers. However, this theoretical model has to be improved for a better coincidence between experimental and

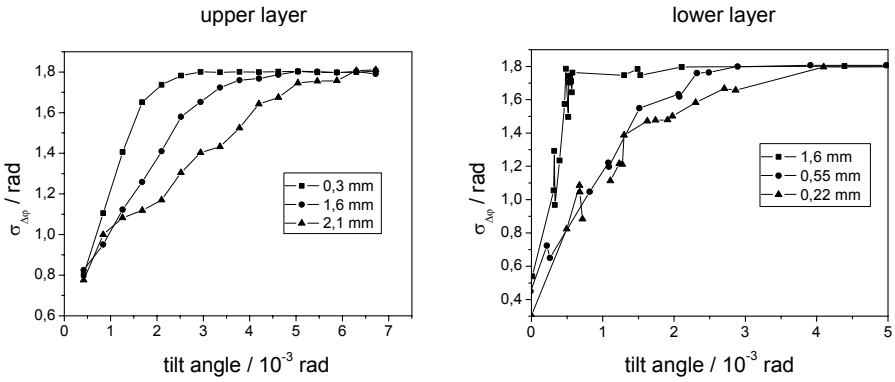

Fig.4. Degradation of mod-2π phase map vs. tilt angle at different distances of layers. Left: tilt of upper layer only. Right: tilt of lower layer only.

theoretical data. As a consequence from this experiments we recognize, that only small deformations are allowed in order to obtain fringe patterns with sufficient contrast.

4. MEASUREMENTS ON COLOURED FRAGMENTS OF TERRACOTTA

In a next step, we performed deformation measurements on original terracotta fragments partly covered with pigmented layers and with dark brownish ground layers of paint. In the following example, we measured on a part of a treated breast armor, which is covered by only two ground layers. Since these layers are very dark and inhomogeneous we first of all performed an OCT measurement to verify that there is enough light reflected from the second layer, which was located about 100µm beneath the surface, to perform a deformation measurement. The fragment was inserted in a climatic box and exposed to several humidity cycles while the resulting deformations were continuously monitored. In Fig. 5 some resulting phase maps representing the deformations of an area of about 1 x 1 mm^2 are shown. The upper two images (Fig.5a and b) are the result of a humidity change from 68% to 73% r.h., while the two lower images (Fig.5c and d) result from a change from 90% to 80% r.h. On the right side (Fig. 5b and d) the measurement of the top layer and on the left side (Fig.5a and c) of the second layer are displayed. A complex structure of separated deformation areas appeared which is best visible in the maps of the top layer, but can also be identified in the maps of the lower layer. These type of deformation showed to be typical throughout all measurements on probes treated with this conservation agent due to the occurrence of a net of micro cracks. The sub-areas undergo bowl-shaped deformation caused by swelling or shrinking of the paint layers.

Of course, in the case of small deformations within the top area, the phase map of the lower layer shows small deformation, too, here less than one fringe (Fig. 5a). Although, the phase maps can be evaluated since the degradation due to de-correlation of the speckle pattern is rather low. The situation tends to get worse if the deformation of the top layer increases. This can be seen in Fig. 5c: the phase map is degraded to such an extend that a reliable evaluation is almost impossible, which of course agrees with the experiments made on the artificial test object. Thus, deformation evaluation is only possible if the image storage rate can be adapted to the actual occurring deformations. Since in our experiment the humidity can be changed as slow as necessary, the deformation measurements are not suffering from

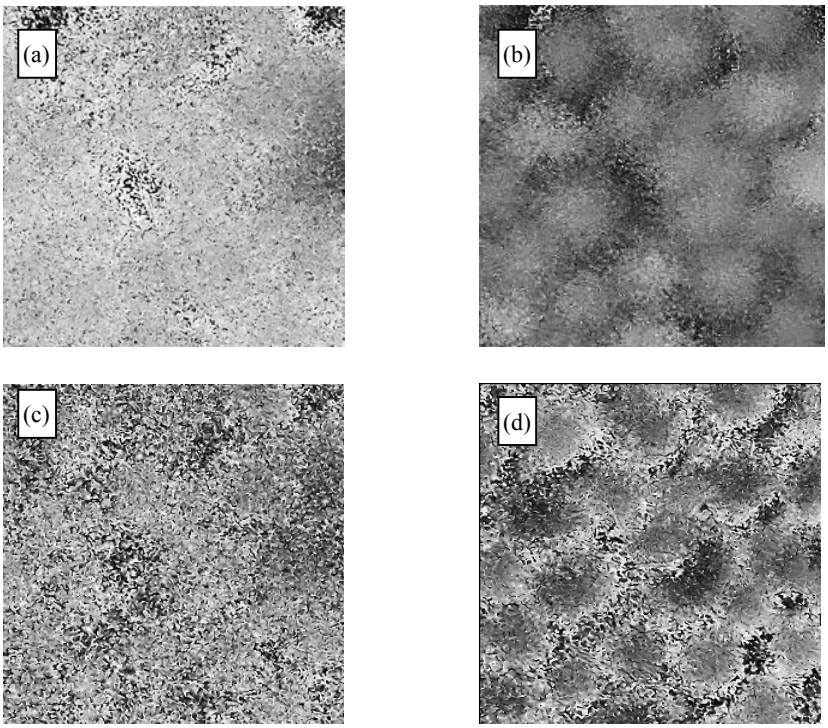

Fig. 5. Deformation measurements on original terracotta fragment. Images (a) and (b) show the deformation during humidity change from 68% to 73% r.h., images (c) and (d) during humidity change from 90% to 80%. On the right side the measurement of the top layer and on the left side the second layer approx. 100µm beneath the top layer are displayed.

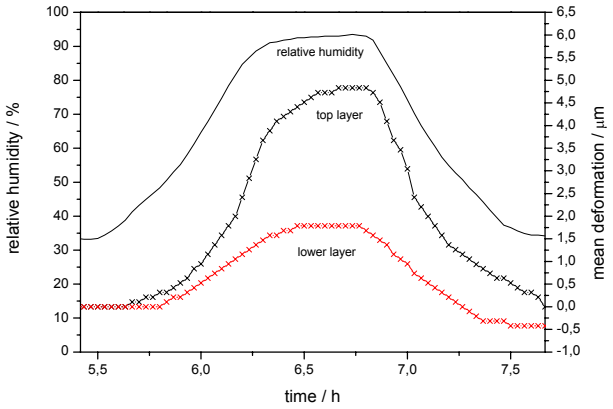

Fig. 6. Mean deformation of top layer and lower layer obtained during a humidity cycle vs. measuring time

this restriction. Images were thus stored after every 30 seconds.

In Fig. 6, the result of a complete humidity cycle is summarized. Here the mean amount of deformation of the upper and the lower layer, as well as the humidity within the climatic box during the cycle is plotted as a function of time. Two main results can be extracted from this measurement: First of all we see, that the upper layer deforms to a maximum extent of about 5 µm, the lower one of about 2µm. Obviously, the lower layer is slightly less affected by the changing humidity, even if we take into account, that the deformation measured for the upper layer is the sum of the deformation of both the layers. Secondly, the time dependence of the deformation of both the layers is equal, which was not expected. That means, that there is no time delay in the reaction of the two layers on the humidity change and hence no damping of the second by the top layer. Probably this can be explained by the existence of the net of micro cracks which enables the direct access of the humidity to the lower paint layer.

5. CONCLUSION

It is shown that the use of a short-coherent superluminescence diode in a standard ESPI system enables depth-selective deformation measurements in layered objects. In addition, the modified method represents a 2-D OCT system, too. Although some restrictions arise in the displacement detection of lower layers due to speckle de-correlation valuable information for the test and optimization of conservation agents can be obtained.

ACKNOWLEDGEMENT

The authors gratefully acknowledge financial support provided by the German Ministry of Education, Science, Research and Technology (BMBF).

REFERENCES

1 K.D. Hinsch and G. Gülker, “Lasers in art conservation”, Phys. World, 37-42, (2001)
2 M.A. Duguay, “Light photographed in flight”, American Scientist, 59, 551-556 (1971)
3 J. G. Fujimoto, W. Drexler, U. Morgner, F. Kärtner, and E. Ippen: Optical Coherence Tomography. Opt. Phot. News, 24-3, (2000).
4 G. Indebetouw and P. Klysubun: “Optical sectioning with low coherence spatio-temporal holography”. Opt. Com.;172: 25-29, (1999).
5 R. Jones and C. Wykes: Holographic and Speckle Interferometry. Cambridge University Press, 1983
6 M. Takeda, H. Ina, S. Kobayashi: Fourier-transform method of fringe pattern analysis for computer-based topography and interferometry, JOSA 72.1, 156-160 (1982).
7 T. Fricke-Begemann und J. Burke, “Speckle interferometry: Three-dimensional deformation field measurement with a single interferogram”, Appl. Opt. 40.28, 5011-5022,(2001).
8 J. Burke and H. Helmers, “Spatial vs. temporal phase shifting: noise comparision in phase maps”, Appl. Opt. 39.25, 4598-4606, (2000).